Multi-physics Design Optimisation of PM-assisted Synchronous Reluctance Motor for Traction Application

Mahir Al-ani
Department of Electrical and Electronic Engineering
University of Nottingham
Nottingham, UK
mahir.al-ani@nottingham.ac.uk

Adam Walker
Department of Electrical and Electronic Engineering
University of Nottingham
Nottingham, UK
adam.walker5@nottingham.ac.uk

Gaurang Vakil
Department of Electrical and Electronic Engineering
University of Nottingham
Nottingham, UK
gaurang.vakil@ nottingham.ac.uk

Ramkumar Ramanathan
Department of Electrical and Electronic Engineering
University of Nottingham
Nottingham, UK
ramanathan.ramkumar@ nottingham.ac.uk

Tianjie Zou
Department of Electrical and Electronic Engineering
University of Nottingham
Nottingham, UK
tianjie.zou@nottingham.ac.uk

Salvatore La Rocca
Department of Electrical and Electronic Engineering
University of Nottingham
Nottingham, UK
salvatore.larocca@nottingham.ac.uk

Antonino La Rocca
Department of Electrical and Electronic Engineering
University of Nottingham
Nottingham, UK
A.larocca@ nottingham.ac.uk

David Gerada
Department of Electrical and Electronic Engineering
University of Nottingham
Nottingham, UK
david.gerada@nottingham.ac.uk

Chris Gerada
Department of Electrical and Electronic Engineering
University of Nottingham
Nottingham, UK
chris.gerada@nottingham.ac.uk

Krzysztof Paciura
Cummins Corporate R&T
Cummins Ltd
Peterborough, UK
krzysztof.paciura@cummins.com

Alastair McQueen
Cummins Corporate R&T
Cummins Ltd
Peterborough, UK
alastair.mcqueens@cummins.com

***Abstract*—Recently, the synchronous reluctance machine limits have been pushed toward meeting the requirements of traction applications. A skilled electromagnetic architecture of a synchronous reluctance machine with the help of permanent magnets can push the limits of power density and speed range to that of traction applications, however, the mechanical integrity of the rotor can still be in question. A traction application means large rotor diameter and high rotational speed, two criteria that makes a challenging design, in particular, mechanically. In this paper, the multi-physics design steps of a permanent magnets assisted synchronous reluctance motor for automotive application, have been presented. Firstly, the electromagnetic design following the size and thermal aspects and constrains has been conducted. Secondly, methods to reduce the mechanical stress has been explored and a bridged mechanical design has been adapted. Finally, thermal analysis of the machine has been conducted to ensure the thermal limits have been satisfied.**

Keywords— Synchronous reluctance, PM assisted, mechanical stress, mechanical design, IPM, traction application, automotive application

I. INTRODUCTION

Attempts to introduce the synchronous reluctance (SynRel) machine to traction application has been reported lately in [1-4]. Obstacles of limited torque-speed range and low power factor have been addressed by including permanent magnets (PMs), i.e. PM assisted synchronous reluctance (PM-SynRel) machine. Compared to the conventional interior permanent magnet (IPM) machine, the PM-SynRel offers higher reluctance torque and therefore higher torque per magnet volume [5]. However, similar to the IPM machine the presence of the PMs adds complicity to the structural design of the rotor when considering the high peripheral speed.

This paper presents a multi-physics design steps of an electric motor for a traction application. The electromagnetic

design started by a detailed parametric optimization. The optimized electromagnetic design (D1) is then mechanically investigated to identify the mechanical challenges and limitations. The mechanical investigation started with studying the debonding of the adhesive that is used to hold the PMs to understand the effect of the adhesive on the structural integrity of the rotor. Following, different methods to reduce the maximum stress to the acceptable material limit were explored, including applying retaining sleeve, and adding internal bridges to hold the PMs. The final design consisted of bridged rotor core to enclose the magnets. The final modified design (D2) is then electromagnetically analysed to evaluate the performance degradation. Finally, thermal analysis of the final electromagnetic and mechanical design (D2) has been conducted to ensure the thermal safety, i.e. satisficing the thermal limits.

II. Design Specifications and Application Requirements

The electric motor is designed for a traction. Such application requires a high torque density along a wide speed range. Table I lists the main design specification and required performance. Fig. 1 presents the torque-speed profile for the peak and continues operation.

Table I Main design specifications and requirements

Parameter	Value
Peak Power (kW)	220
Peak Time (s)	30
Peak Torque (Nm)	750
Ideal Continuous Power (kW)	150
Acceptable Continuous Power (kW)	130
Ideal Continuous Torque (Nm)	511
Acceptable Continuous Torque (Nm)	444
Base Speed (rpm)	2800
Max Speed (rpm)	15000
Max Winding Temp (°C)	180
DC Link Voltage Range (V)	620 to 760
DC Link Voltage Rated (V)	660
Target Mass (kg)	140
Target Minimum Efficiency (%)	95
Laminated steel	HXT780T
PM grade	N38UH, Br 1.26T

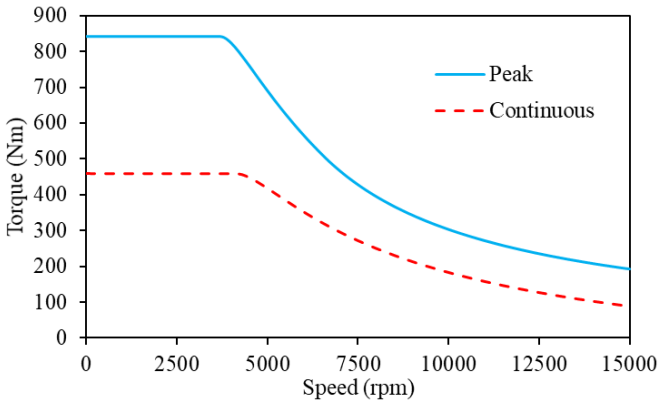

Fig. 1 Torque-speed profile of the peak and continuous operation.

III. Electromagnetic Design (D1)

The PM-SynRel topology has been globally optimized using generic algorithm for defined objective functions. Table II lists the optimization constrains, degrees of freedom and objectives. Fig. 2 presents the machine geometrical parameters included in the optimization. The final electromagnetically optimized designed machine (D1) is shown in Fig. 3.

Table II Optimized parameters

Parameter	Value
Constrains	
Outer diameter (mm)	300
Axial length (mm)	300
Airgap length (mm)	1.8
Degrees of freedom	
Split ratio	0.4-0.7
Slot height (mm)	10-20
Back-iron thickness (mm)	10-20
1st layer magnet fill percentage	0-100
2nd layer magnet fill percentage	0-100
3rd layer magnet fill percentage	0-100
Number of turns per coil	7-15
Number of parallel paths	1, 5, and 10
Objectives	
Peak power (kW)	≥250
Efficiency	≥94
PM mass (kg)	≥7
Machine mass (kg)	≥140
Torque ripple	≤10

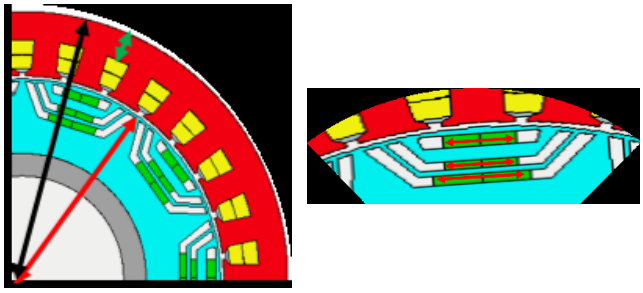

Fig. 2 Optimized design parameters.

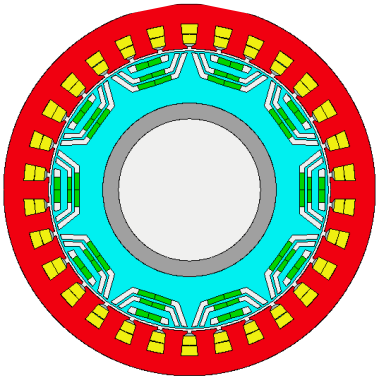

Fig. 3 Electromagnetically optimized design (D1).

IV. Mechanical Design (D2)

Using FEA, the rotor of D1 has been studied and redesigned to ensure mechanical safety. The boundary condition is a fixed inner surface of the rotor, whereas the load is a rotation speed of 16.5krpm, i.e. 10% speed safety margin. Table III lists the properties of the rotor core and magnets. The maximum allowed stress in the rotor is set to 720MPa allowing an extra 10% stress safety margin.

Table III Comparison of SPM, IPM and SynRel-PM.

Parameter	Steel	PM
Mass density (kg/m^3)	7650	7500
Young's modulus (MPa)	200	160
Poisson's ratio	0.3	0.3
Yield strength (GPa)	800	60

A. Debonding

Initially, the adhesive strength has been evaluated to obtain if the adhesive would experience a debonding or not. Therefore, the magnet contact with the rotor core has been set to bonded contact with adhesive properties. It is worth noting that although using a stronger adhesive will maintain the bond between the magnet and core, the PM will experience a high stress that would surpass the yield limit strength of the PMs. Fig. 4 presents the stress distribution in the rotor when the contact are bonded and debonded. Fig. 5 presents the bottom magnet contact maximum equivalent (von-Mises) stress and maximum deformation at different rotor speeds, it can be seen at low speed, i.e. 5000rpm, the cohesive strength between the steel and magnet on the inner magnet surface has failed. The debonding between the magnets and the core which results in significantly high mechanical stress at the rotor outer bridges.

(a) Bonded (b) Debonded

Fig. 4 Mechanical stress destitution in the rotor.

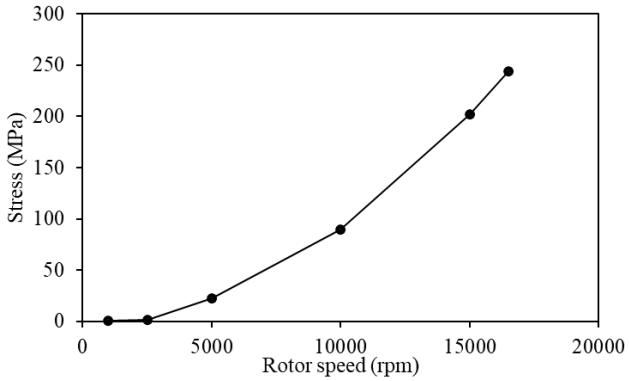

(a) Maximum stress

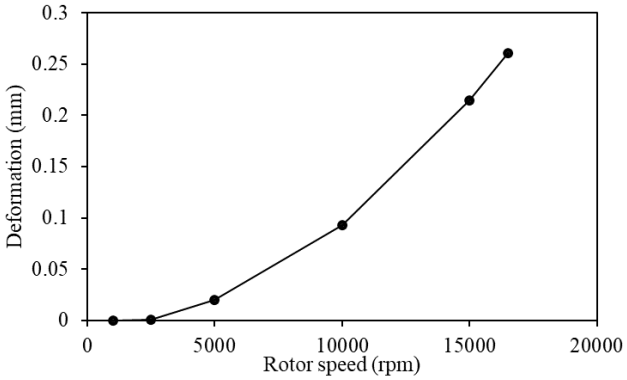

(b) Maximum deformation

Fig. 5 Adhesive contact performance at different rotor speeds.

B. Sleeve

A 0.8mm thick carbon fibre retaining sleeve has been applied to the rotor with an interference fit of 0.08mm. Fig. 6 presents the stress distribution of the rotor at speed of 16.5krpm. Although the maximum stress has been reduced from 2915MPa to 2570Mpa.

Although the sleeve has managed to reduce the maximum stress by decreasing the deformation along the magnets, the reduction is relatively small. Using thicker sleeve with higher interface fit by reducing the rotor outer frame thickness, i.e. 3mm sleeve with 0.3mm interference fit, has reduced the stress further, however, 1979MPa still significantly higher than the limit. In addition, manufacturing difficulties are expect to assemble a 0.3mm interference fit sleeve. These reasons making the sleeve infeasible for this design.

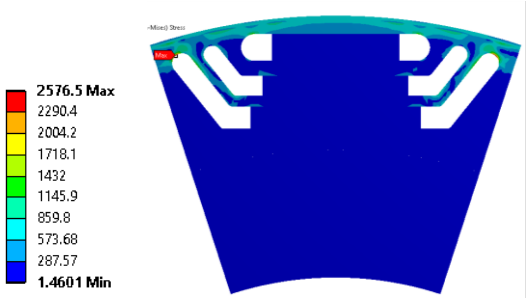

(a) Stress, 0.8mm sleeve, 0.08mm interference fit

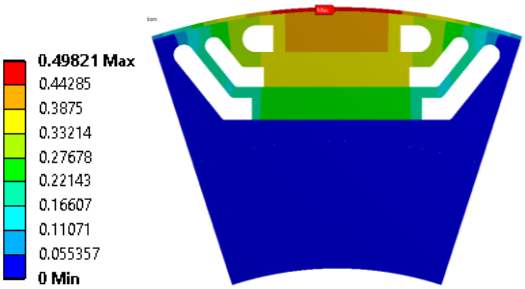

(b) Deformation, 0.8mm sleeve, 0.08mm interference fit

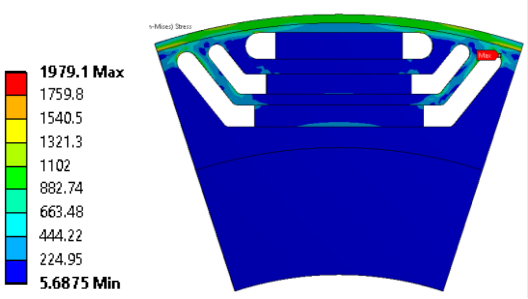

(c) Stress, 3mm sleeve, 0.3mm interference fit

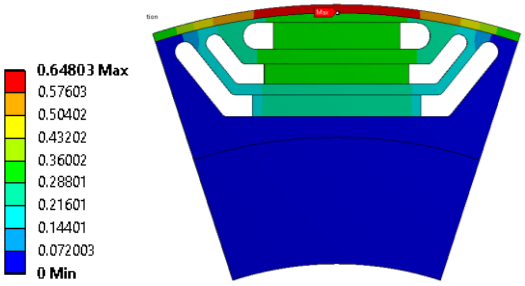

(d) Deformation, 3mm sleeve, 0.3mm interference fit

Fig. 6. Stress and deformation of the rotor D1 with carbon fiber sleeve.

C. *Brdiges*

By observing the stress and deformation in the rotor, Fig. 7, it can be seen that the highest deformation occurs at the centre line of the rotor, this places a high stress on the outer frame. Therefore, retain the central line of the rotor is expected to reduce the stress.

Firstly, bridges at both sides of the magnets were added. Although the maximum stress reduced, the large deformation along the central line is still high and therefore, the stress still high as shown in Fig. 8. Bridges along the central line were added in addition to the side bridges. The magnets have been segmented into two parts separated by bridges to reduce the deformation at the middle line, side bridges are added to lock the magnets in their location and avoid any magnet slipping. Fig. 9 shows the rotor stress and deformation, since the maximum stress has been reduced to 590MPa which is lower than the limit of the safety limit of the material.

Further changes are conducted to maintain the rotor stress within the acceptable limit and minimize the bridges thicknesses to enhance the electromagnetic performance. Fig. 9 presents the four different iterations together with their stress and deformation. The iterations include shaping and reducing the bridges thicknesses. The final design (D2) is shown in Fig. 9 (fourth iteration).

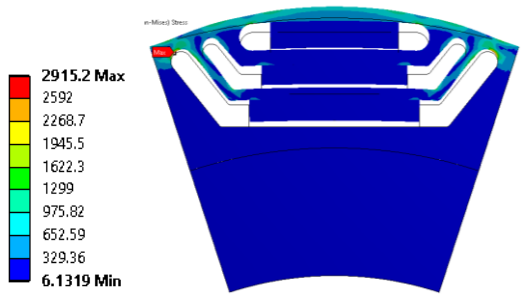

(a) Stress

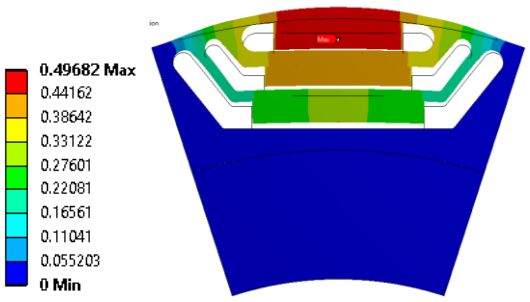

(b) Deformation

Fig. 7. Stress and deformation of the D1 design.

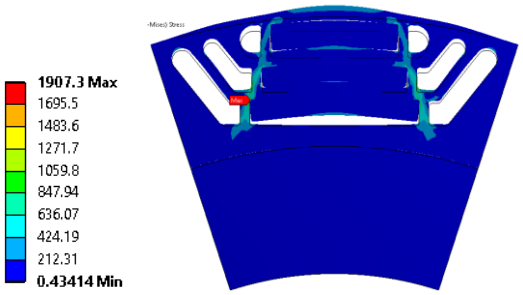

(c) Stress

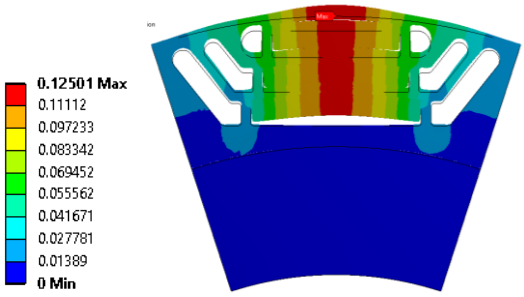

(d) Deformation

Fig. 8. Stress and deformation of the D1 design with side bridges.

V. INVESTGATING THE ELECTROAMGETNIC PERFORMANCE

The D2 has been analysed electromagnetically, as expected, the bridges creates short-circuit paths for the PM flux. Therefore, a reduction in the performance has been observed. However, the initial electromagnetic design (D1) has been over-designed, i.e. the torque-speed characteristics are higher than that of the target shown in Fig.1. This is to take in consideration any possible performance degradation comes from mechanical designing. Therefore, the mechanically

modified design (D2) has satisfactory torque-speed curve. As a result, not changes are required. Fig. 10 presents the torque-speed characteristics of the D1 and D2 designs.

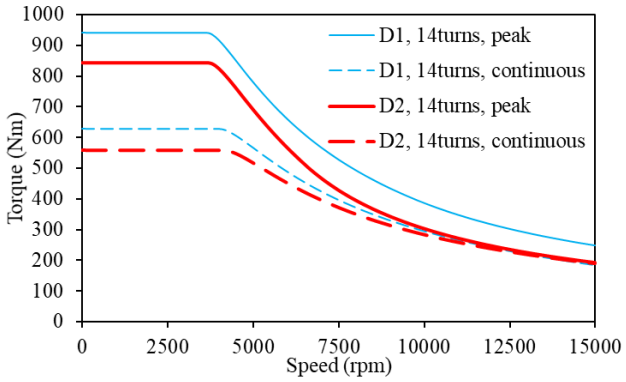

(a) Torque-speed curve

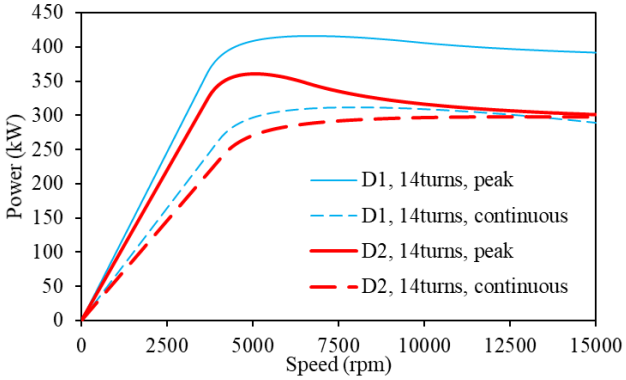

(b) Power-speed curve

Fig. 9. Torque-speed characteristics of the D1 and D2 machines.

VI. Thermal Analysis

Using LPC, thermal analysis of the D2 has been conducted to ensure thermal safety. Cooling jacket with a 9.6L/min flow rate, 65°C inlet temperature and EGW50/50 fluid has been used. A duty cycle of 30 second peak condition, i.e. maximum losses at peak operation, has been employed. Fig. 11 presents the temperature at different parts of the machine and Table IV lists the temperature in the different machine parts. Since the thermal performance satisfy the design requirements, no changes for the design are needed.

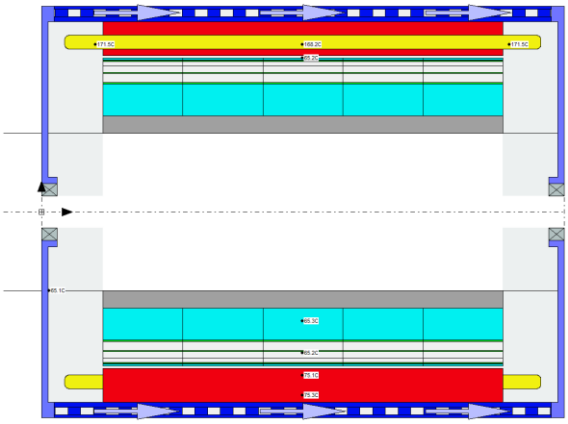

Fig. 10. Thermal layout and temperatures in different parts of D3 at 30second peak condition.

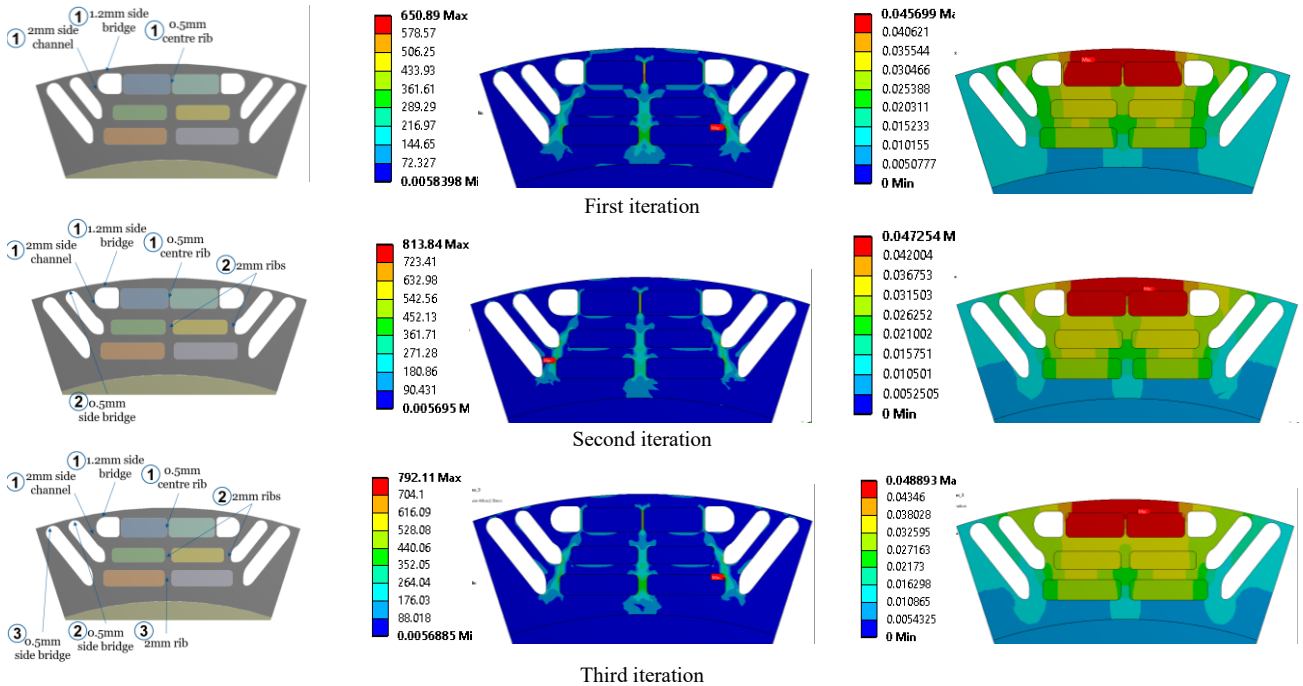

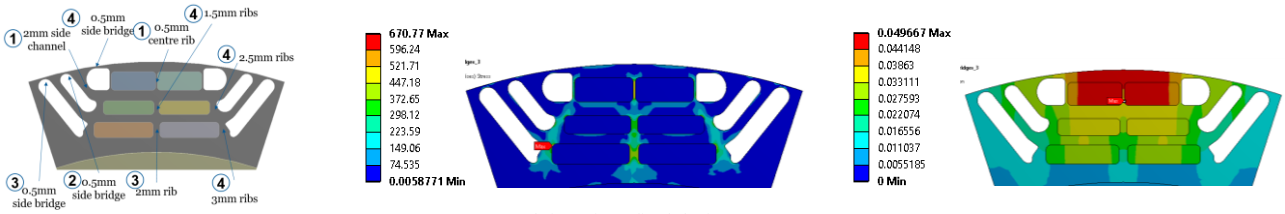

(a) Rotor layout and changes aplied

Forth iteration (final design D3)

(b) Stress (c) Deformation

Fig. 11. Stress and deformation of the different iteration of D1 design with middle and side bridges.

Table IV Temperatures of different machine parts.

Machine part	Temperature (°C), Peak	Temperature (°C), Continuous
Winding	168.2	107.4
End-winding	171.5	109.7
Rotor surface	65.2	65.1
Rotor yoke	65.3	65
Magnets	65.2	65
Stator tooth	75.9	68.2
Stator yoke	75.3	68

VII. Comparsion with Different PM Topologies

Other PM topologies have been explored to obtain the most suitable topology for the application requirements. Surface-mounted PM (SPM) machine with halbach magnetic orientation can meet the performance targets, however, the need for large quantity of rounded and diagonal magnets and thick retaining sleeve, as shown in Fig. 12 (a). Similarly, interior PM (IPM) machine requires large magnet quaintly to meet the target, Fig. 12 (b) presents the IPM topology. Therefore, PM-SynRel topology has been selected since this topology can meet the targets with the lowest PM material quantity. Table V compares the three topologies.

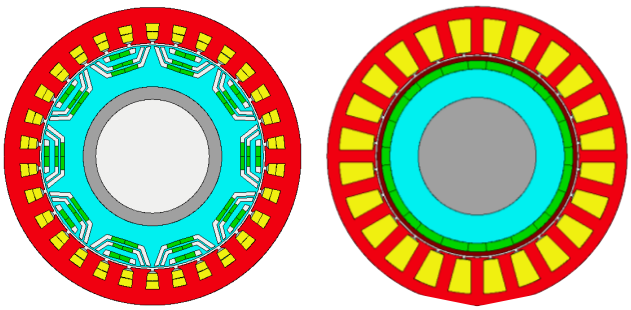

(a) PM-SynRel (b) SPM

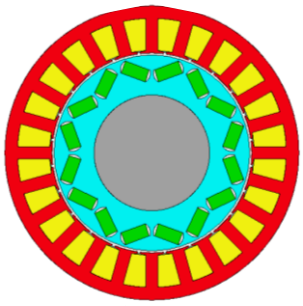

(c) IPM

Fig. 12 SPM and IPM machine topologies.

Table V Comparison of SPM, IPM and PM-SynRel.

Parameter	PM-SynRel (a)	SPM (b)	IPM (c)
PM Mass	6.8	14.3	12.6
Mass	122	136	117
Stack Length	306	400	330

VIII. Conclusion

This paper presents a multi-physics designing steps of a high torque density PM-SynRel electric motor designed for automotive application. The design procedure started with optimizing the design parameters using global multi-objective optimization. This step generated the first electromagnetically designed model D1 which achieved all the required targets. Following, mechanical investigation and designing of the rotor conducted to ensure mechanical safety. Mechanical bridges on the PM sides and middle have been employed, this design referred to by D2. This technique managed to reduces the mechanical stress from 2900MPa to the limit of 670MPa. As a result, a reduction in the electromagnetic results have been observed due to the short circuit flux paths generated by the bridges. Thermal analysis have then been conducted to ensure the machine operates within the safe temperature limits. Finally, a comparison with SPM and IPM machines has been conducted to highlight the benefits of using PM-SynRel topology.

References

[1] N. Bianchi, S. Bolognani, E. Carraro, M. Castiello and E. Fornasiero, "Electric Vehicle Traction Based on Synchronous Reluctance Motors," in IEEE Transactions on Industry Applications, vol. 52, no. 6, pp. 4762-4769, Nov.-Dec. 2016.

[2] K. Grace, S. Galioto, K. Bodla and A. M. El-Refaie, "Design and Testing of a Carbon-Fiber-Wrapped Synchronous Reluctance Traction Motor," in IEEE Transactions on Industry Applications, vol. 54, no. 5, pp. 4207-4217, Sept.-Oct. 2018.

[3] P. B. Reddy, A. M. El-Refaie, S. Galioto and J. P. Alexander, "Design of Synchronous Reluctance Motor Utilizing Dual-Phase Material for Traction Applications," in IEEE Transactions on Industry Applications, vol. 53, no. 3, pp. 1948-1957, May-June 2017.

[4] M. D. Nardo, G. L. Calzo, M. Galea and C. Gerada, "Design Optimization of a High-Speed Synchronous Reluctance Machine," in IEEE Transactions on Industry Applications, vol. 54, no. 1, pp. 233-243, Jan.-Feb. 2018.

[5] Z. Q. Zhu, W. Q. Chu and Y. Guan, "Quantitative comparison of electromagnetic performance of electrical machines for HEVs/EVs," in CES Transactions on Electrical Machines and Systems, vol. 1, no. 1, pp. 37-47, March 2017.